

Saturation spectra of low lying states of Nitrogen revisited

Thomas Carette¹, Messaoud Nemouchi², Per Jönsson³ and Michel Godefroid¹

¹ Service de Chimie quantique et Photophysique, CP160/09,

Université Libre de Bruxelles, Avenue F.D. Roosevelt 50, B 1050 Brussels, Belgium

² Laboratoire d'Électronique Quantique, Faculté de Physique, USTHB, BP32, El-Alia, Algiers, Algeria

³ Center for Technology Studies, Malmö University, 205-06 Malmö, Sweden

Received: March 19, 2019/ Revised version:

Abstract. The hyperfine constants of the levels $2p^2(^3P)3s\ ^4P_J$, $2p^2(^3P)3p\ ^4P_J^o$ and $2p^2(^3P)3p\ ^4D_J^o$, deduced by Jennerich et al. [1] from the observed hyperfine structures of the transitions $2p^2(^3P)3s\ ^4P_J \rightarrow 2p^2(^3P)3p\ ^4P_J^o$, and $2p^2(^3P)3s\ ^4P_J \rightarrow 2p^2(^3P)3p\ ^4D_J^o$, recorded by saturation spectroscopy in the near-infrared, strongly disagree with the *ab initio* values of Jönsson et al. [2]. We propose a new interpretation of the recorded weak spectral lines. If the latter are indeed reinterpreted as crossover signals, a new set of experimental hyperfine constants is deduced, in very good agreement with the *ab initio* predictions.

PACS. PACS-key 31.15.aj, 31.30.Gs, 32.10.Fn – PACS-key 78.47.N

1 Introduction

In 1943, Holmes [3] measured the isotope shifts (IS) of the $2p^2(^3P)3s\ ^4P_J \rightarrow 2p^2(^3P)3p\ ^4P_J^o$, $2p^2(^3P)3s\ ^2P_J \rightarrow 2p^2(^3P)3p\ ^2P_J^o$, and $2p^2(^3P)3s\ ^4P_J \rightarrow 2p^2(^3P)3p\ ^4S_J^o$ transitions for the ^{15}N – ^{14}N isotopic pair. He observed a surprising variation of the IS from one multiplet component to another of the same transition. Cangiano et al. [4] later confirmed this effect by measuring the hyperfine structure constants and isotope shifts of the $2p^2(^3P)3s\ ^4P_J \rightarrow 2p^2(^3P)3p\ ^4P_J^o$ transitions using an external cavity diode laser and Doppler-free techniques. More recently, the hyperfine structures of these near-infrared transitions have been remeasured by Jennerich et al. [1], also using saturation absorption spectroscopy but improving the spectral resolution. In the same work, the authors completed this study by investigating the structure of $2p^2(^3P)3s\ ^4P_J \rightarrow 2p^2(^3P)3p\ ^4D_J^o$ transitions around 870 nm. Values of the hyperfine structure coupling constants of all the upper and lower multiplets were obtained for both isotopes. Isotope shifts of three transitions in each multiplet were also measured and the significant J -dependence of the shifts was confirmed. The authors appealed for further theoretical investigation to confirm the observations.

In response to this, Jönsson et al. [2] calculated the electronic hyperfine factors using elaborate correlation models. The resulting *ab initio* hyperfine constants disagree completely with the experimental parameters obtained by fitting the observed hyperfine spectra [1]. This disagreement calls for a reinterpretation of the experimental spectral lines.

The saturated-absorption spectroscopy is a Doppler-free method which measures the absorption of a probe beam in an atomic vapor cell saturated by a counter-propagating pump beam. The absorption spectrum of the probe beam featured several Lamb-dips with a width of the order of the natural width. When the Doppler-broadened line spreads on several transitions, as for instance in hyperfine spectra, crossover signals often appear when the pump and probe laser beams frequency corresponds to the average of the frequencies of two hyperfine transitions [5]. A crossover signal might then show up in a spectrum between hyperfine lines sharing either the lower level or the upper level (involving three levels), or none of them (involving four levels) [6, 7]. In the former case, if the common level is the lower one, the two beams propagating through the atomic vapor both contribute in reducing its population. The probe beam absorption then weakens, like the absorption hyperfine lines. This corresponds to a positive intensity crossover. If the common level is the upper one, the probe beam absorption signal may either increase or decrease [6, 7]. If the probe beam absorption spectrum is resolved and strong enough, crossover signals might be helpful in identifying unambiguously the hyperfine lines [8]. More frequently, their presence complicates the spectral analysis due to possible overlaps with the hyperfine components themselves. Moreover, the theory of crossover intensities is rather complex. A sign inversion of the crossover intensities has been observed in the hyperfine spectrum of the sodium D1 line with a change of the vapor temperature [9]. Saturation effects, optical pumping [10, 11, 12, 13], radiation pressure [14], pump and probe beam-polarizations [15], may also affect the intensities of hyperfine lines and crossover signals. Recent progress has been

achieved in saturated absorption spectroscopy to eliminate crossovers in hyperfine spectra. The hyperfine structure spectrum of the rubidium D2 line has been so measured [16] using a vapor nano-cell. The same spectrum, measured in saturated absorption spectroscopy, with co-propagating pump and probe laser beams of the same intensity, is also free of crossovers [17].

While the strong hyperfine lines are relatively easy to identify, the weak components are usually not. The existence of crossover resonances as a consequence of the saturated absorption technique was recognized in only two transitions studied by Jennerich *et al.* [1]. In the present work, we completely revisit their saturation spectra, calling their line assignments in question. Starting from the fact that the strong mismatch between observation and theory only concerns the weak hyperfine lines (see section 2), we reinterpret most of them as crossover signals (see section 3). The extracted new set of experimental hyperfine constants is consistent with the *ab initio* results of Jönsson *et al.* [2].

2 Hyperfine spectra simulations

The hyperfine structure of a spectrum is caused by the interaction of the angular momentum of the electrons (\mathbf{J}) and of the nucleus (\mathbf{I}), forming the total atomic angular momentum $\mathbf{F} = \mathbf{I} + \mathbf{J}$. Neglecting the higher order multipoles as well as the off-diagonal effects, the energy W_F of a hyperfine level, characterized by the quantum number F associated to \mathbf{F} , is

$$W_F = W_J + A \frac{C}{2} + B \frac{3C(C+1) - 4I(I+1)J(J+1)}{8I(2I-1)J(2J-1)} \quad (1)$$

with $C = F(F+1) - I(I+1) - J(J+1)$. W_J is the energy of the fine structure level J . A and B are the hyperfine constants that describe respectively the magnetic dipole and electric quadrupole interactions.

Giving A and B in MHz, the frequency of a hyperfine transition between two levels (JF) and ($J'F'$) is:

$$\nu = \nu_0 + a'A' + b'B' - aA - bB \quad (2)$$

where the primed symbols stand for the upper level. ν_0 is the frequency of the $J'-J$ transition. The factors a and b (a' and b') are the coefficients that weight the hyperfine constants A and B (A' and B') in formula (1), i.e.

$$a = \frac{C}{2} \quad ; \quad b = \frac{3C(C+1) - 4I(I+1)J(J+1)}{8I(2I-1)J(2J-1)} \quad (3)$$

To be consistent with [1], we simulate the spectra using Lorentzian line shapes with a width of 100 MHz, which is of the order of magnitude of the experimental linewidth. The relative intensities of the hyperfine lines I_r are deduced from the formula [18]

$$I_r = (2F+1)(2F'+1) \left\{ \begin{matrix} J & I & F \\ F' & 1 & J' \end{matrix} \right\}^2 \quad (4)$$

We do not simulate the crossovers in the spectral synthesis, except for one specific transition (Figure 6).

The total nuclear angular momentum I of the isotopes ^{15}N and ^{14}N are equal to $\frac{1}{2}$ and 1, respectively. The nuclear quadrupole moment Q is non zero for the isotope ^{14}N only, $Q(^{14}\text{N}) = +0.02001(10)$ b [19]. The nuclear magnetic moments of the isotopes are $\mu_I(^{15}\text{N}) = -0.28318884(5)$ nm and $\mu_I(^{14}\text{N}) = +0.40376100(6)$ nm [19]. The expected ratio between the magnetic hyperfine constants characterizing a given J -level of the two isotopes should be

$$A_J(^{15}\text{N})/A_J(^{14}\text{N}) = \frac{\mu_I(^{15}\text{N})I(^{14}\text{N})}{\mu_I(^{14}\text{N})I(^{15}\text{N})} = -1.4028 \quad (5)$$

Table 1 presents the *ab initio* hyperfine constants A and B of Jönsson *et al.* [2], obtained from elaborate multiconfigurational Hartree-Fock calculations with relativistic corrections, together with the experimental ones of Jennerich *et al.* [1]. As concluded in [2], the huge and systematic disagreement between observation and theory appeals for further investigations. We compare those two sets through their corresponding spectral simulations. Figures 1(a,b) and 2(a,b) display the simulated spectra for transitions $3s \ ^4P_{5/2} \rightarrow 3p \ ^4P_{3/2,5/2}^o$ in both isotopes ^{15}N and ^{14}N . The plain lines correspond to the synthetic spectra using the *ab initio* constants from [2] and the dashed lines to the ones using the original experimental constants from [1]. We denote these two spectra \mathcal{S}_t and \mathcal{S} , respectively. For the spectra based on the *ab initio* hyperfine parameters, we add a t -subscript to the letters a, b, c, ..., characterizing the transitions (Figures 1(c,e) and 2(c,e)). One sees that the disagreement between the theoretical and experimental hyperfine constants observed in Table 1 reduces to a disagreement for the weak lines positions, while the intense lines of both simulated spectra agree satisfactorily.

The recorded spectra of Jennerich *et al.* [1] (Fig. 1(d) and 2(d)) and their assignments (illustrated in the hyperfine level diagrams 1(c,e) and 2(c,e)) are also displayed for the two transitions $3s \ ^4P_{5/2} \rightarrow 3p \ ^4P_{3/2,5/2}^o$. From the diagram corresponding to the transition $^4P_{5/2} \rightarrow ^4P_{3/2}^o$ of ^{15}N , one realizes that the lines b and c have a common upper level. It means that a crossover could appear at a frequency $(\nu_b + \nu_c)/2$. In Figure 1(a), the line b of the simulated experimental spectra could be reinterpreted as a crossover signal of lines b_t and c_t of the theoretical spectrum. Why the crossover signal $b = \text{co}(b_t, c_t)$ appears while the real line b_t does not show up, is unclear. Likewise, the experimental line b of the ^{14}N spectrum can be reinterpreted as the crossover of a_t and b_t while e would be the crossover of c_t and e_t . The same argument applies to all low intensity lines of the experimental spectra of the transitions $^4P_{5/2} \rightarrow ^4P_{3/2,5/2}^o$ and $^4P_{5/2} \rightarrow ^4D_{3/2,5/2,7/2}^o$. Note that the hyperfine level diagrams of the transitions $^4P_{5/2} \rightarrow ^4D_{3/2,5/2}^o$ differ from those of $^4P_{5/2} \rightarrow ^4P_{3/2,5/2}^o$ only by their upper level spacing, but their spectra look very similar.

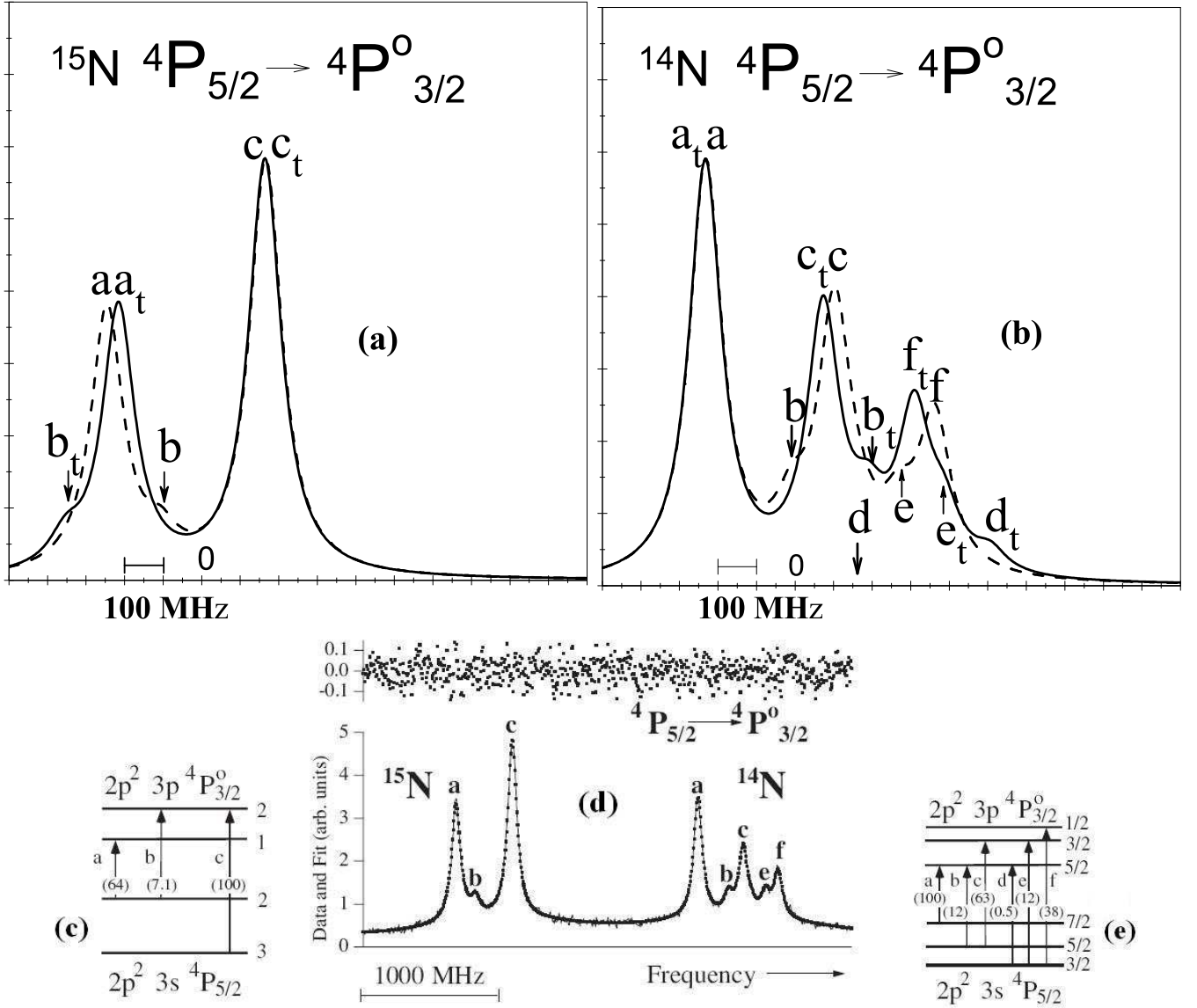


Fig. 1. (a,b): Hyperfine spectra, without the crossover, of the transition $4P_{5/2} \rightarrow 4P^o_{3/2}$ simulated with the experimental constants of Jennerich et al. [1] (dashed lines) and the *ab initio* constants of Jönsson et al. [2] (plain lines). For the latter, a *t*-subscript is added to the line symbol. (d): original recorded spectra of Jennerich et al. [1]. (c) and (e): level diagrams and line assignments from Jennerich et al. [1].

In the following section, we show that the *ab initio* hyperfine constants [2] of the states $4P^o_{3/2,5/2}$, $4D^o_{3/2,5/2,7/2}$ and $4P_{5/2}$ are compatible with the recorded spectra of Jennerich et al. [1], at the condition that we identify the low intensity lines as crossover signals. We also confirm the intense hyperfine line's identification. We then discuss the hyperfine spectra corresponding to the transitions $4P_{3/2} \rightarrow 4P^o_{1/2}$ and $4P_{1/2} \rightarrow 4D^o_{1/2}$, which are analyzed differently. A new set of “experimental” hyperfine constants is then deduced and used to compare the unresolved experimental spectra $4P_{1/2} \rightarrow 4P^o_{3/2}$, $4P_{3/2} \rightarrow 4P^o_{3/2}$ and $4P_{3/2} \rightarrow 4P^o_{5/2}$ to the theoretical simulations.

3 Interpretation of the weak lines in terms of crossovers

The procedure to deduce a new set of experimental hyperfine constants is based on the transition frequencies obtained from the original set of hyperfine constants of Jennerich et al. [1] using equation (2). The residuals (data minus fit) obtained by Jennerich et al. [1] - such as those displayed in their Fig. 2 - are systematically neglected in the extracted line frequencies. Those residuals being small (about 4% of the most intense line) and rather featureless, this procedure should be reliable enough. We also use as such the experimental error bars of [1] to estimate the uncertainties of the present set of hyperfine constants. At this stage, the latter only indicate the limits of our model

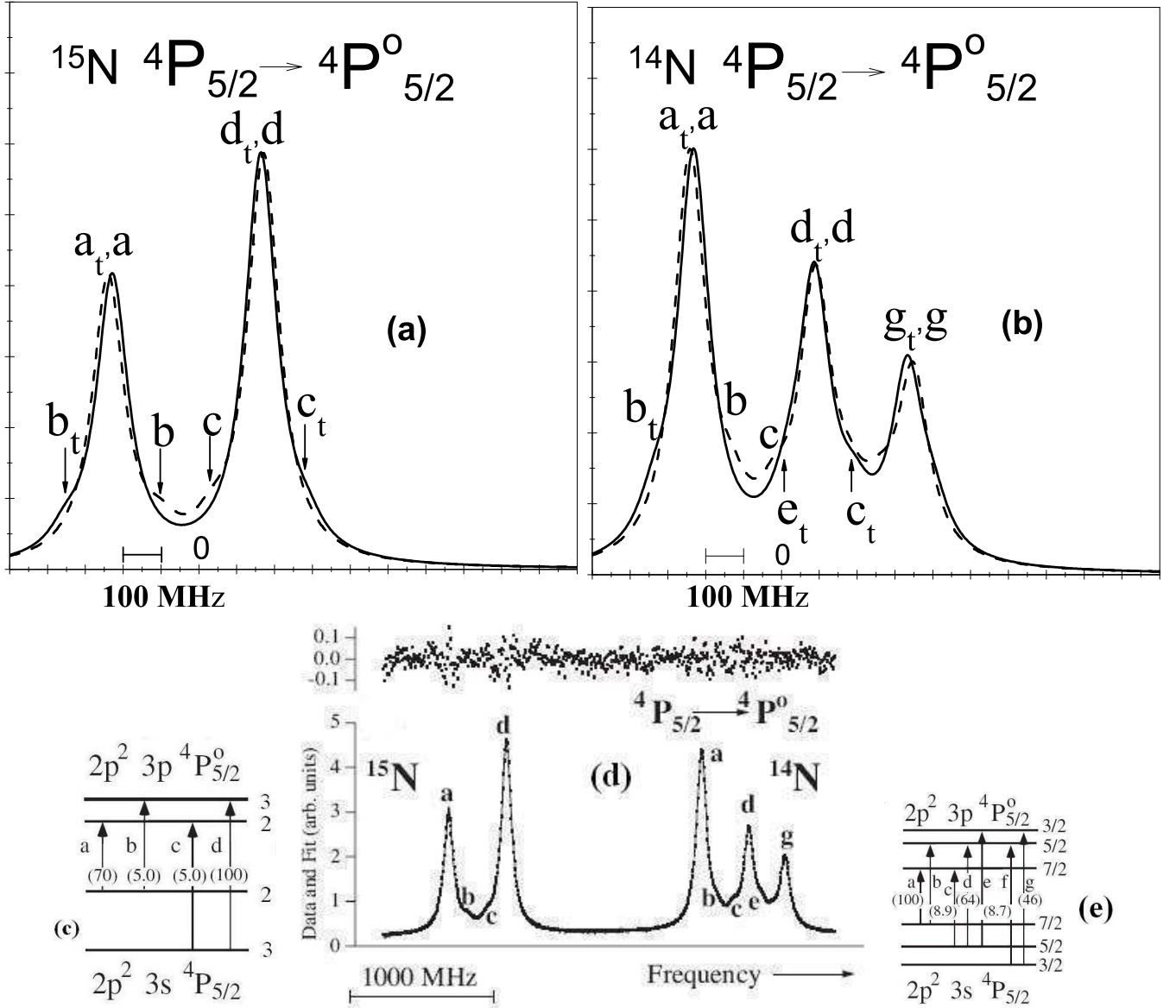


Fig. 2. (a,b): Hyperfine spectra, without the crossover, of the transition $^4P_{5/2} \rightarrow ^4P^o_{5/2}$ simulated using the experimental constants of Jennerich et al. [1] (dashed lines) and the *ab initio* constants of Jönsson et al. [2] (plain lines). For the latter, a *t*-subscript is added to the line symbol. (d): original recorded spectra of Jennerich et al. [1]. (c) and (e): level diagrams and line assignments from Jennerich et al. [1].

and should be definitely refined through a final fit of the recorded spectra on the basis of the present analysis. Finally, in our model, we use the observed relative intensities (4) only to distinguish the “strong” from the “weak” hyperfine components.

3.1 ^{15}N : $^4P_{5/2} \rightarrow ^4P^o_{3/2,5/2}$ and $^4P_{5/2} \rightarrow ^4D^o_{3/2,5/2,7/2}$

The hyperfine spectra corresponding to the transitions $^4P_{5/2} \rightarrow ^4P^o_{3/2,5/2}$ and $^4P_{5/2} \rightarrow ^4D^o_{3/2,5/2,7/2}$ of ^{15}N have two intense lines and one or two weak lines. The intense lines do not share any hyperfine level. Their frequency are given by the formula (2), where the quadrupole term vanishes ($I = 1/2$). Let us set the frequency of the center of

gravity of the experimental spectrum \mathcal{S} to zero, and also define the \mathcal{S}_c spectrum simulated with a new set of hyperfine constants that we want to determine. The *c* subscript stands for the reassignment of the weak measured lines to crossovers. By defining $\delta\nu_0$ as the center of gravity of this latter spectrum and denoting ν_1 and ν_2 the frequencies of two intense lines in the two \mathcal{S} and \mathcal{S}_c spectra, one has

$$\nu_1 = a'_1 A'_e - a_1 A_e = \delta\nu_0 + a'_1 A' - a_1 A, \quad (6)$$

$$\nu_2 = a'_2 A'_e - a_2 A_e = \delta\nu_0 + a'_2 A' - a_2 A \quad (7)$$

where A'_e and A_e (A' and A) are respectively the hyperfine constants of the upper and lower levels, in the \mathcal{S} (\mathcal{S}_c) spectrum.

The frequency ν_3 of the experimental hyperfine line interpreted as a crossover signal in the \mathcal{S}_c spectrum and sharing the upper state with the intense line ν_2 , verifies

$$\nu_3 = a'_2 A'_e - a_1 A_e = \delta\nu_0 + a'_2 A' - \frac{a_1 + a_2}{2} A. \quad (8)$$

Equations (6), (7) and (8) form a well defined system of three linear equations for the unknown A' , A and $\delta\nu_0$. Solving it, we get

$$A = 2A_e, \quad (9)$$

$$A' = A'_e + \frac{a_1 - a_2}{a'_1 - a'_2} A_e, \quad (10)$$

$$\delta\nu_0 = \frac{a'_1 a_2 - a_1 a'_2}{a'_1 - a'_2} A_e. \quad (11)$$

The new values of the hyperfine constants (A and A') of the states involved in the transitions $^4P_{5/2} \rightarrow ^4P_{3/2,5/2}^o$ and $^4P_{5/2} \rightarrow ^4D_{3/2,5/2,7/2}^o$, presented in Table 1, are in good agreement with the *ab initio* values for all the considered states.

Figures 3(a) and 3(d) display the spectra simulated with the new constants A' and A (plain line) and the original experimental one (dashed line) for two hyperfine multiplets. We use the *c*-subscript to label the \mathcal{S}_c lines. It should be pointed out that Jennerich et al. [1] wrongly inverted the intensities of the hyperfine lines *b* ($F = 3 \rightarrow F' = 4$) and *c* ($F = 3 \rightarrow F' = 3$) in the level diagram of the transition $^4P_{5/2} \rightarrow ^4D_{7/2}^o$. Moreover, line *c* should have been labeled *b* in Figure 2(g) of their article. Finally, the upper level of line *a* should be $F' = 3$ instead of $F' = 4$ contrarily to what the hyperfine level diagram of their Figure 4(e) indicates.

From equation (11) we also deduce the center of gravity $\delta\nu_0$ of the different fine structure transitions. We obtain $\delta\nu_0 = 0$ for the transitions $^4P_{5/2} \rightarrow ^4P_{5/2}^o$, $^4D_{5/2}^o$ ($J = J'$), $\delta\nu_0 = -11.34(9)$ MHz for $^4P_{5/2} \rightarrow ^4P_{3/2}^o$, $^4D_{3/2}^o$ and $\delta\nu_0 = 5.67(5)$ MHz for $^4P_{5/2} \rightarrow ^4D_{7/2}^o$.

3.2 ^{14}N : $^4P_{5/2} \rightarrow ^4P_{3/2,5/2}^o$ and $^4P_{5/2} \rightarrow ^4D_{3/2,5/2,7/2}^o$

The case of isotope ^{14}N is slightly complicated by the non-vanishing electric quadrupolar interaction, but the presence of three well identified lines permits us to perform the same analysis. If ν_1 , ν_2 and ν_3 are the intense line frequencies, their assignment gives :

$$\begin{aligned} \nu_1 &= a'_1 A'_e + b'_1 B'_e - a_1 A_e - b_1 B_e \\ &= \delta\nu_0 + a'_1 A' + b'_1 B' - a_1 A - b_1 B, \end{aligned} \quad (12)$$

$$\begin{aligned} \nu_2 &= a'_2 A'_e + b'_2 B'_e - a_2 A_e - b_2 B_e \\ &= \delta\nu_0 + a'_2 A' + b'_2 B' - a_2 A - b_2 B, \end{aligned} \quad (13)$$

$$\begin{aligned} \nu_3 &= a'_3 A'_e + b'_3 B'_e - a_3 A_e - b_3 B_e \\ &= \delta\nu_0 + a'_3 A' + b'_3 B' - a_3 A - b_3 B. \end{aligned} \quad (14)$$

If amongst the observed weak lines of a given spectrum, ν_4 and ν_5 are identified as crossover signals, one has two additional constraints :

$$\begin{aligned} \nu_4 &= a'_2 A'_e + b'_2 B'_e - a_1 A_e - b_1 B_e \\ &= \delta\nu_0 + a'_2 A' + b'_2 B' - \frac{a_1 + a_2}{2} A - \frac{b_1 + b_2}{2} B, \end{aligned} \quad (15)$$

$$\begin{aligned} \nu_5 &= a'_3 A'_e + b'_3 B'_e - a_2 A_e - b_2 B_e \\ &= \delta\nu_0 + a'_3 A' + b'_3 B' - \frac{a_2 + a_3}{2} A - \frac{b_2 + b_3}{2} B. \end{aligned} \quad (16)$$

As for isotope ^{15}N , new experimental hyperfine constants A' , A , B' , B and the center of gravity $\delta\nu_0$ of the considered transition are determined from

$$A = 2A_e \quad (17)$$

$$\begin{aligned} A' &= A'_e - D^{-1} \\ &\times \{A_e [a_1(b'_2 - b'_3) + a_2(b'_3 - b'_1) + a_3(b'_1 - b'_2)] \\ &+ B_e [b_1(b'_2 - b'_3) + b_2(b'_3 - b'_1) + b_3(b'_1 - b'_2)]\} \end{aligned} \quad (18)$$

$$B = 2B_e \quad (19)$$

$$\begin{aligned} B' &= B'_e - D^{-1} \\ &\times \{A_e [a_1(a'_2 - a'_3) + a_2(a'_3 - a'_1) + a_3(a'_1 - a'_2)] \\ &+ B_e [b_1(a'_2 - a'_3) + b_2(a'_3 - a'_1) + b_3(a'_1 - a'_2)]\} \end{aligned} \quad (20)$$

$$\delta\nu_0 = \frac{\alpha A_e + \beta B_e}{D} \quad (21)$$

where

$$\begin{aligned} D &= a'_1(b'_2 - b'_3) + a'_2(b'_3 - b'_1) + a'_3(b'_1 - b'_2), \\ \alpha &= a_1(a'_2 b'_3 - a'_3 b'_2) + a_2(a'_3 b'_1 - a'_1 b'_3) + a_3(a'_1 b'_2 - a'_2 b'_1), \\ \beta &= b_1(a'_2 b'_3 - a'_3 b'_2) + b_2(a'_3 b'_1 - a'_1 b'_3) + b_3(a'_1 b'_2 - a'_2 b'_1). \end{aligned}$$

The so-deduced values of A' , A , B' and B are given in Table 1. They are in good agreement with the *ab initio* theoretical hyperfine constants. Like above, Figures 3(c) and 3(f) present the hyperfine spectra of the two transitions $^4P_{5/2} \rightarrow ^4P_{5/2}^o$, $^4D_{7/2}^o$ for the isotope ^{14}N .

We find $\delta\nu_0 = 0$ for the transitions $^4P_{5/2} \rightarrow ^4P_{5/2}^o$, $^4D_{5/2}^o$, $\delta\nu_0 = 21.68(17)$ MHz for $^4P_{5/2} \rightarrow ^4P_{3/2}^o$, $^4D_{3/2}^o$ and $\delta\nu_0 = -10.84(9)$ MHz for $^4P_{5/2} \rightarrow ^4D_{7/2}^o$.

One should expect the quadrupole hyperfine constant B of the state $^4D_{3/2}^o$ to be rather small. Indeed, in the context of hyperfine simulations based on the Casimir formula and in the non-relativistic approximation, the main contribution to the B constants is given by [20] :

$$B_J = -G Q b_q \frac{6\langle \mathbf{L} \cdot \mathbf{J} \rangle^2 - 3\langle \mathbf{L} \cdot \mathbf{J} \rangle - 2L(L+1)J(J+1)}{L(2L-1)(J+1)(2J+3)} \quad (22)$$

where $G = 234.96475$ is used for obtaining B_J in MHz when expressing the quadrupole moment Q in barns, the hyperfine parameter b_q in a_0^{-3} and with

$$\langle \mathbf{L} \cdot \mathbf{J} \rangle = \frac{1}{2} [J(J+1) + L(L+1) - S(S+1)]. \quad (23)$$

It is easily verified that equation (22) vanishes for the $^4D_{3/2}^o$ state of ^{14}N . Therefore, a non-zero $B(^4D_{3/2}^o)$ value

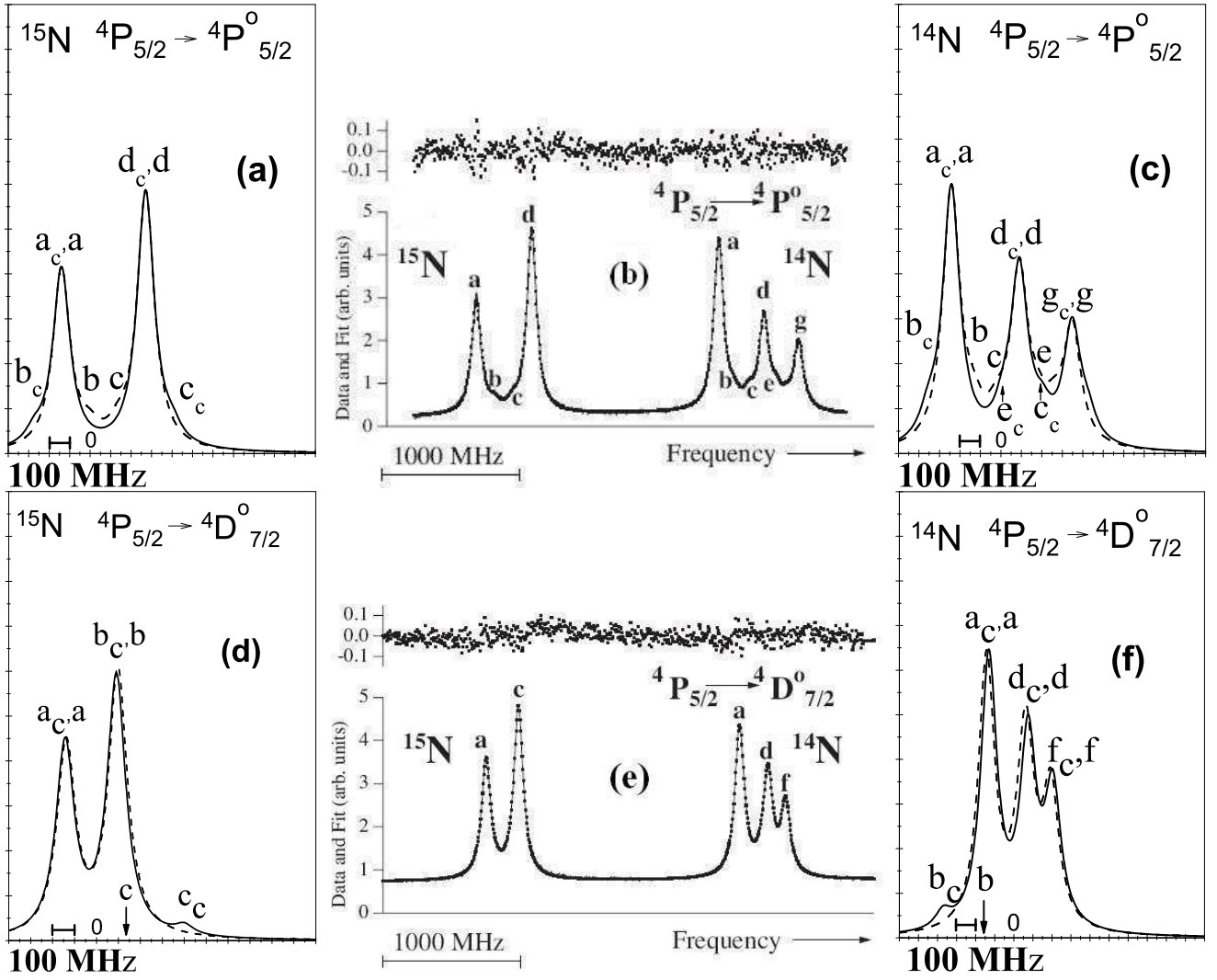


Fig. 3. ^{15}N and ^{14}N simulated (sides) and recorded [1] (middle) spectra of the transitions $^4\text{P}_{5/2} \rightarrow ^4\text{P}^o_{5/2}$ and $^4\text{P}_{5/2} \rightarrow ^4\text{D}^o_{7/2}$. The plain line corresponds to the S_c spectrum simulation (transitions labels with subscripts c), without the crossovers, and the dashed line corresponds to the S simulated spectrum using the experimental hyperfine constants of Jennerich et al. [1]. The simulations are superposed on the same scale with the center of gravity of each spectra being at the origin (*i.e.* not including the $\delta\nu_0$ shift).

should be interpreted as arising from higher order relativistic effect and/or in terms of hyperfine interaction between levels of different J . From the present analysis, we deduce $B(^4\text{D}^o_{3/2}) = -0.9(17)$ MHz, which is from this point of view, more realistic than the experimental value $(+10.46(88)$ MHz) reported in [1].

3.3 The transition $^4\text{P}_{1/2} \rightarrow ^4\text{D}^o_{1/2}$

The spectrum of the transition $^4\text{P}_{1/2} \rightarrow ^4\text{D}^o_{1/2}$ of isotope ^{15}N is resolved (Figure 4(b)) but the lines a ($F = 1 \rightarrow F' = 0$) and c ($F = 0 \rightarrow F' = 1$) have the same relative intensities (50% of the most intense line). It causes an *a priori* ambiguous assignment. The same problem appears in the ^{14}N spectrum where lines a ($F = 1/2 \rightarrow F' = 3/2$) and d ($F = 3/2 \rightarrow F' = 1/2$) have the same relative inten-

sities (80% of the most intense line). Line c ($F = 1/2 \rightarrow F' = 1/2$, 10%) is not helpful since it does not appear in this spectrum. Because of this identification problem, Jennerich et al. [1] suggested two possible values for each of the hyperfine constants of the $^4\text{P}_{1/2}$ and $^4\text{D}^o_{1/2}$ states (see Table 1). The first proposition corresponds to the case where the $\nu_a < \nu_c$ for ^{15}N and $\nu_a < \nu_d$ for ^{14}N . The second proposition corresponds to the inverse situation. On the basis of the presence of a crossover with a positive intensity between lines b and d in the spectrum of ^{14}N , Jennerich et al. [1] estimated that the first proposition is the most likely. Indeed, they infer from the presence of this crossover that b and d share their lower level, leading to the identification of the lines a and d . The same argument was used for ^{15}N using the crossover between a and b . A similar argument has been used in previous studies of Chlorine [21] and Oxygen [22]. However, a crossover

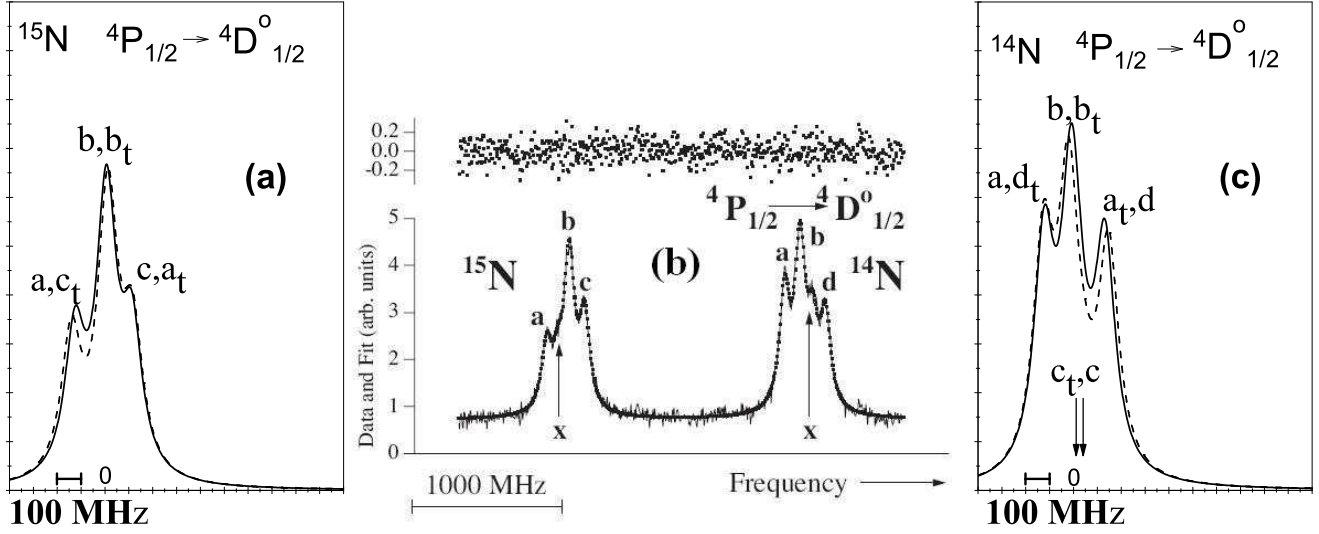


Fig. 4. ^{15}N and ^{14}N simulated (sides) and recorded [1] (middle) spectra of the transition $^4\text{P}_{1/2} \rightarrow ^4\text{D}^o_{1/2}$. The plain line corresponds to the simulated spectrum, without the crossovers, using the *ab initio* hyperfine constants of Jönsson et al. [2] (transitions labels with subscripts *t*). The dashed line corresponds to the simulated spectrum using the experimental hyperfine constants of Jennerich et al. [1]. The simulations are superposed on the same scale with the center of gravity of each spectra being at the origin (*i.e.* not including the $\delta\nu_0$ shift).

arising from two transitions with a common *upper* level may also have a positive intensity [6,7]. Combining this observation with the fact that the agreement between the hyperfine constants of the states $^4\text{P}_{1/2}$ and $^4\text{D}^o_{1/2}$ and the *ab initio* values [2] is much better with the second set than with the first one, we think that the first choice of Jennerich et al. [1] is not the good one, and we definitely opt for the second one. Figures 4(a) and 4(c) display the simulated spectra using the *ab initio* constants calculated by Jönsson et al. [2] (plain line) and the experimental ones favoured by Jennerich et al. [1] (dashed line)¹ for both isotopes.

3.4 The transition $^4\text{P}_{3/2} \rightarrow ^4\text{P}^o_{1/2}$

The recorded transition spectra of $^4\text{P}_{3/2} \rightarrow ^4\text{P}^o_{1/2}$ is showed in Figure 5(b). For the ^{15}N spectrum, with two well identified lines (*a* and *c*) and an experimental line *b* that we interpret as a crossover signal of b_t and c_t , we applied the same procedure described above, using equations (9)-(11). The new constants $A' = A(^4\text{P}^o_{1/2})$ and $A = A(^4\text{P}_{3/2})$ that we infer are reported in Table 1 ($\delta\nu_0 = -11.98(12)$ MHz). Simulated spectra are presented in Figure 5(a). The experimental set of hyperfine constants of Jennerich et al. [1] and the present one generate simulated spectra that do not agree as well as for the above discussed transitions. This relative disagreement can be attributed to the fact that the reassigned “weak” line is, as in

the other spectra, much weaker than expected from equation (4) and that the line *b* of the transition $^4\text{P}_{3/2} \rightarrow ^4\text{P}^o_{1/2}$ (20% of the most intense line) is strong enough to perturb deeply the *a* line shape. For this, we refer to the section 4.2 of Jennerich et al. [1] who discussed the possibility of observing line shape perturbation in some transitions, in particular when the separation of two lines is comparable to the natural linewidth. Furthermore, the presence of a crossover between a_c and b_c would affect the center of the peak and therefore increase the experimental hyperfine constants error.

This problem appears even more seriously in the case of ^{14}N . Indeed, the transition $^4\text{P}_{3/2} \rightarrow ^4\text{P}^o_{1/2}$ cannot be analysed according to section 3.2. The hyperfine spectrum of this transitions is composed of only one well identified line (*a*:100%, $\nu_1=5/2 \rightarrow 3/2$), three nearly equally intense lines (*b*:30%, $\nu_2=3/2 \rightarrow 3/2$; *d*:37%, $\nu_4=3/2 \rightarrow 1/2$; *e*:30%, $\nu_5=1/2 \rightarrow 1/2$), one line which is too weak to be visible (*c*:3.7%, $\nu_3=1/2 \rightarrow 3/2$) and possibly many crossovers. Trusting our line assignment for the same spectrum in ^{15}N , it is unlikely that the experimental line *b* could be anything else than a crossover of a hyperfine transition with the most intense line. We suppose

$$\begin{aligned} \nu_1 &= a'_1 A'_e + b'_1 B'_e - a_1 A_e - b_1 B_e \\ &= \delta\nu_0 + a'_1 A' + b'_1 B' - a_1 A - b_1 B, \end{aligned} \quad (24)$$

$$\begin{aligned} \nu_2 &= a'_1 A'_e + b'_1 B'_e - a_2 A_e - b_2 B_e \\ &= \delta\nu_0 + a'_1 A' + b'_1 B' - \frac{a_1 + a_2}{2} A - \frac{b_1 + b_2}{2} B. \end{aligned} \quad (25)$$

On the other hand, the transition $\nu_3=1/2 \rightarrow 3/2$ is too weak to be observed and the identification of the transitions $\nu_4=3/2 \rightarrow 1/2$ et $\nu_5=1/2 \rightarrow 1/2$ are uncertain. The observed peak in the region of those lines is interpreted as their superposition with their crossovers. It is therefore

¹ Note that the simulations based on the experimental hyperfine constants that we favour would have strictly the same shape as the dashed lines of Figure 4(a) and 4(c) but with inverted transitions labels (*a,c*) and (*a,d*) respectively.

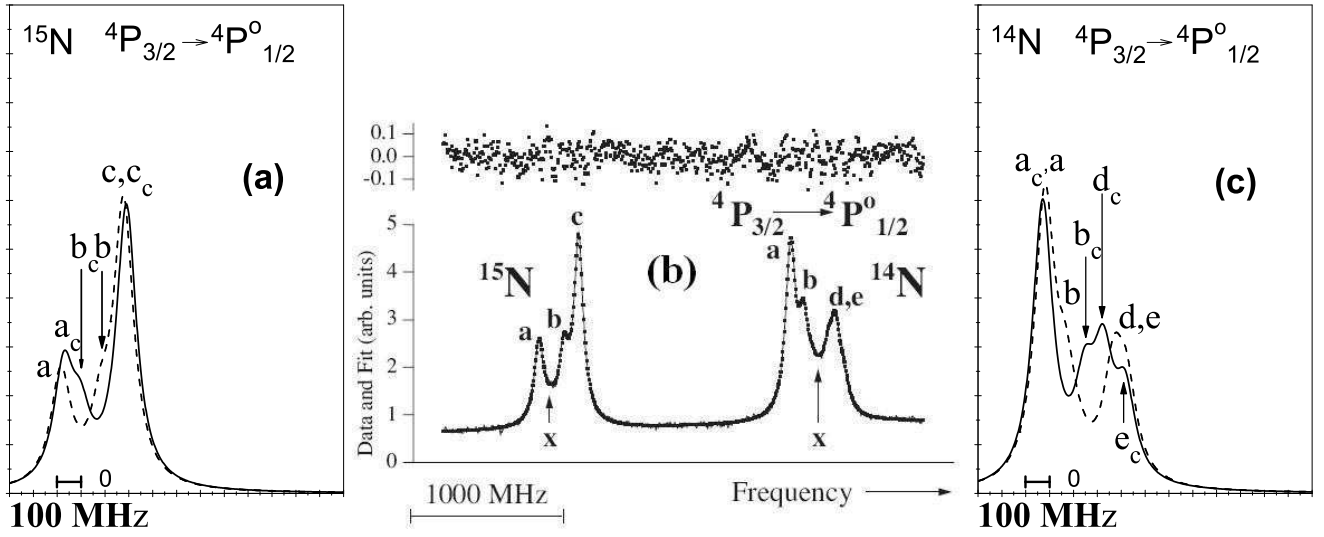


Fig. 5. ^{15}N and ^{14}N simulated (sides) and recorded [1] (middle) spectra of the transition $^4\text{P}_{3/2} \rightarrow ^4\text{P}^o_{1/2}$. The plain line corresponds to the \mathcal{S}_c spectrum simulation, without the crossover, based on the experimental hyperfine structure constants determined in the present work (transitions labels with subscripts c). The dashed line corresponds to the \mathcal{S} calculated spectrum using the experimental hyperfine constants of Jennerich *et al.* [1]. The simulations are superposed on the same scale with the center of gravity of each spectra being at the origin (*i.e.* not including the $\delta\nu_0$ shift).

impossible to extract the hyperfine constant A' from the available experimental data.

Nonetheless, neglecting in the simulation a crossover signal between these transitions introduces an error on the ν_4 and ν_5 lines that we denote respectively ϵ_{ν_4} and ϵ_{ν_5} . We have

$$\begin{aligned} \nu_4 &= \epsilon_{\nu_4} + a'_2 A'_e - a_2 A_e - b_2 B_e \\ &= \delta\nu_0 + a'_2 A' - a_2 A - b_2 B \end{aligned} \quad (26)$$

$$\begin{aligned} \nu_5 &= \epsilon_{\nu_5} + a'_2 A'_e - a_3 A_e - b_3 B_e \\ &= \delta\nu_0 + a'_2 A' - a_3 A - b_3 B \end{aligned} \quad (27)$$

These four constraints permit to express the hyperfine constants involved in this transition as a function of ϵ_{ν_4} and ϵ_{ν_5} :

$$A' = A_{1/2}(^4\text{P}^o) = -74.8(34) - \frac{2}{3}\epsilon_{\nu_4} \quad (28)$$

$$A = A_{3/2}(^4\text{P}) = 61.79(95) - \frac{1}{6}(\epsilon_{\nu_4} - \epsilon_{\nu_5}) \quad (29)$$

$$B = B_{3/2}(^4\text{P}) = 16.54(82) + \frac{1}{3}(\epsilon_{\nu_4} - \epsilon_{\nu_5}) \quad (30)$$

$$\delta\nu_0 = 14.60(29) + \frac{1}{6}(\epsilon_{\nu_4} + \epsilon_{\nu_5}) \quad (31)$$

If we impose $A(^{15}\text{N}) = -1.4028 A(^{14}\text{N})$ to get A and A' in the reinterpreted set of hyperfine constants, we have $B_{3/2}(^4\text{P}) = 3.5(91)$ MHz, $\epsilon_{\nu_4} = -36.0(75)$ MHz, $\epsilon_{\nu_5} = 3(18)$ MHz and $\delta\nu_0 = 9.1(44)$ MHz. Figure 5(c) displays the simulated spectrum of this transition with the new constants.

In Figure 6, we finally tempt a crude spectral synthesis including the three crossover signals $\text{co}(a, b)$, $\text{co}(b, d)$ and $\text{co}(d, e)$, adopting a negative intensity for the first one (common lower level) and positive intensities for the two

others (common upper level). The absolute intensity values are estimated from the average of the two hyperfine relative intensities calculated according to equation (4). The theoretical spectrum (plain line) agrees satisfactorily with the “observed” one (dashed line).

3.5 Transitions $^4\text{P}_{3/2} \rightarrow ^4\text{P}^o_{5/2}$ and $^4\text{P}_{1/2} \rightarrow ^4\text{P}^o_{3/2}$

The hyperfine spectra of the transitions $^4\text{P}_{3/2} \rightarrow ^4\text{P}^o_{5/2}$ and $^4\text{P}_{1/2} \rightarrow ^4\text{P}^o_{3/2}$ were also recorded by Jennerich *et al.* [1]. Our simulated spectra are compared with the measured ones in Figures 7(a,b,c,d). The spectrum of the transition $^4\text{P}_{3/2} \rightarrow ^4\text{P}^o_{5/2}$ simulated with the experimental hyperfine constants determined by Jennerich *et al.* [1] (dashed line) indicates that the measured spectrum should be resolved while it is not in reality. There is another contradiction between the synthetic and experimental spectra for the transition $^4\text{P}_{1/2} \rightarrow ^4\text{P}^o_{3/2}$ of isotope ^{14}N . There is indeed an asymmetry in the measured line that suggests the presence of a low intensity line to the *left* of it (see the lower spectrum of Figure 7(a)), while the experimental hyperfine constant set tends to predict it to the *right* (see the upper spectrum of Figure 7(a)). To explain this discrepancy between simulations and observations, the authors suggested that strong line shape perturbation could appear in these transitions in a saturation spectroscopy experiment (*cf.* section 4.2 of [1]). To the contrary, the simulations based on the present reinterpretation (plain line of Figures 7(c,d)) are in agreement with the non-resolved spectra and small features in those lines are assigned.

The only measurement of the spectra of the transition $^4\text{P}_{3/2} \rightarrow ^4\text{P}^o_{3/2}$ was recorded by Cangiano *et al.* [4] but no figure is presented for it. Figures 8(a,b) display the sim-

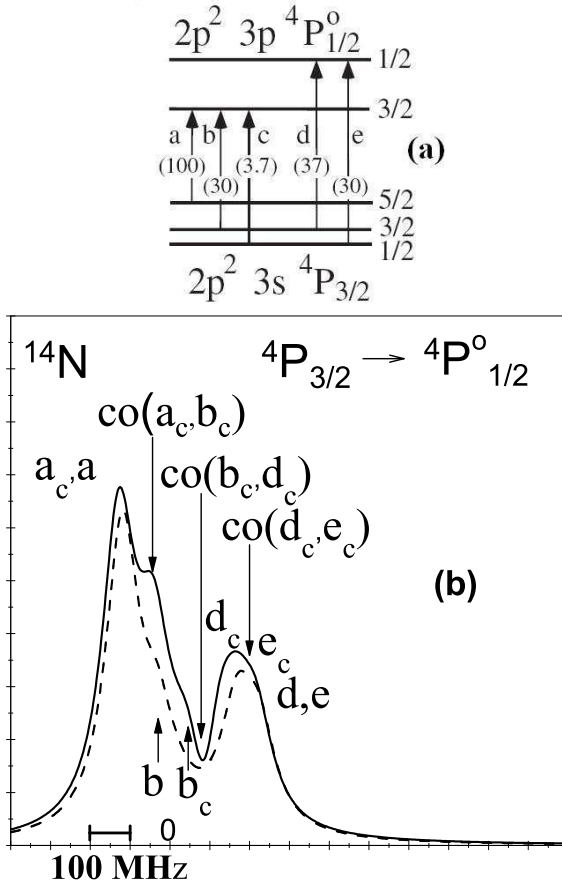


Fig. 6. Synthetic spectra of the transition $4P_{3/2} \rightarrow 4P_{1/2}^o$. The plain line corresponds to the S_c simulation (transitions labels with indices c) including the three most intense crossover (co) signals in the simulation (see text). The dashed line corresponds to the S calculated spectrum using the experimental hyperfine constants of Jennerich et al. [1], without the crossovers. The simulations are superposed on the same scale with the center of gravity of each spectra being at the origin (*i.e.* not including the $\delta\nu_0$ shift). Note the consistency with the recorded spectra of Figure 5.

ulated spectra using both Jennerich et al.'s experimental (dashed line) and present (plain line) sets of hyperfine constants. The resulting spectra are respectively resolved and unresolved.

4 J -dependent specific mass shifts in $3s\ ^4P \rightarrow 3p\ ^4L^o$ transitions

The isotope shift (IS) of a transition is often separated in three contributions : the normal mass shift (NMS), linear in the line frequency, the specific mass shift (SMS), which is proportional to the change of the mass polarization term expectation value between the two levels involved in the transition

$$\Delta \left\langle \sum_{i < j} \mathbf{p}_i \cdot \mathbf{p}_j \right\rangle, \quad (32)$$

and the field shift (FS), which depends on the variation of the electron density inside the nuclear charge distribution. Using the wave functions of [2], the latter contribution is estimated to about 0.2 MHz in the considered transitions and is therefore neglected in the present work. The level specific mass shift difference between two fine structure components J' and J of a same LS term can be obtained by measuring the transition IS from these states to a common $L'S'J'$ level.

Upper levels $3p\ ^4P^o$ and $3p\ ^4D^o$: Cangiano et al. [4] found some J -dependency for the upper $3p\ ^4P^o$ term SMS. They obtained 110(300) MHz and 318(300) MHz for the SMS differences $5/2 - 3/2$ measured relatively to $3s\ ^4P_{5/2}$ and $3s\ ^4P_{3/2}$, respectively. Holmes [3] predicted a compatible shift of 51(33) MHz. Only the value of Cangiano et al. obtained with respect to the level $3s\ ^4P_{5/2}$ overlaps with the experimental results of Jennerich et al. [1] who found a negative difference of $-32.0(32)$ MHz (see Table 2). In the case of the $3p\ ^4D^o$ term, Jennerich et al. measured $-14.7(2.5)$ MHz for the $7/2 - 5/2$ levels SMS difference.

As suggested in section 3, the results of Cangiano et al. [4] and Jennerich et al. [1] are affected by a wrong assignment of the spectral lines, inducing an error $\delta\nu_0$ on the fine structure transitions center. Adopting the present interpretation of the observed spectra, the SMS values are revised from the sum of the IS and $\delta\nu_0$, with their uncertainties (see last column of Table 2). The error estimation on the SMS values is likely optimistic and should ultimately be refined from a proper fit of the recorded spectra. It is however useful within the limits exposed in the beginning of section 3.

We observe from the third column of Table 2 a remarkably small J - and L -dependency of the SMS for the odd $3p\ ^4L_J^o$ upper states, in agreement with limited relativistic *ab initio* calculations that estimate a J -dependency of maximum 1 MHz.

As discussed in section 3.5, we predict unresolved spectra, as observed, for $3s\ ^4P_J \rightarrow 3p\ ^4P_{J'}^o$, with $(J, J') = (1/2, 3/2), (3/2, 3/2)$ and $(3/2, 5/2)$ (see Figure 7 and 8), while Jennerich et al. [1] explained the absence of expected structure by invoking strong line shape perturbations. Therefore, the shifts for these lines could be more meaningful than originally thought. However, a fit of the original spectra for those transitions is needed to assure a more precise determination of their SMS.

Lower level $4P$: Holmes measured a value of $-240(68)$ MHz for the SMS difference $4P_{5/2} - 3/2$ using the two transitions sharing the common $3p\ ^4S_{3/2}^o$ level [3]. For the same difference, Cangiano et al. measured $-553(300)$ MHz and $-344(300)$ MHz using $3p\ ^4P_{5/2}^o$ and $3p\ ^4P_{3/2}^o$, respectively [4]. As revealed by the last column of Table 2, all the SMS values for the $3s\ ^4P_{5/2} \rightarrow 3p\ ^4L_J^o$ transitions lie in a window of $-2746(3)$ MHz. Assuming that the SMS value differs weakly between the fine structure levels $3p\ ^4L_J^o$, as discussed above, we obtain about -167 MHz for the level

Table 2. Transition specific mass shifts (in MHz). Comparison between the values deduced from Jennerich et al.’s analysis [1] (second column) with the values deduced from the S_c spectra (present analysis - see text). The field shift is neglected.

Transition	ref. [1]	This work
$3s\ ^4P_{1/2} \rightarrow 3p\ ^4D_{1/2}^o$	-2488.1(15)	-2488.1(15)
$3s\ ^4P_{3/2} \rightarrow 3p\ ^4P_{1/2}^o$	-2558.3(22)	-2579.4(68)
$3s\ ^4P_{5/2} \rightarrow 3p\ ^4D_{5/2}^o$	-2748.17(84)	-2748.17(84)
$3s\ ^4P_{5/2} \rightarrow 3p\ ^4D_{7/2}^o$	-2762.9(16)	-2746.4(18)
$3s\ ^4P_{5/2} \rightarrow 3p\ ^4P_{3/2}^o$	-2713.4(14)	-2746.4(17)
$3s\ ^4P_{5/2} \rightarrow 3p\ ^4P_{5/2}^o$	-2745.4(18)	-2745.4(18)

SMS difference $3s\ ^4P(5/2 - 3/2)$ and about -91 MHz for $(3/2 - 1/2)$.

This relatively large J -dependency can be explained by the well known strong mixing between $1s^2\ 2s^2\ 2p^2\ 3s\ ^4P$ and $1s^2\ 2s\ 2p^4\ ^4P$ [2,23]. Indeed, the inspection of the Breit-Pauli eigenvectors obtained in relatively large correlation spaces reveals that the weight of the $1s^2\ 2s\ 2p^4\ ^4P$ component (≈ 0.3) increases by about 1% from $J = 1/2$ to $J = 3/2$ levels, and by 2% from $J = 3/2$ to $J = 5/2$. These changes of eigenvector compositions are most likely reliable since they well reproduce the observed fine structure (within 2%). We conclude that the $3s\ ^4P$ J -dependency of the wave functions can be estimated neglecting the term mixing of different LS -symmetries and is largely dominated by the relativistic effects on the $3s\ ^4P$ correlation.

5 Conclusion

We completely revisited the analysis of the near-infrared hyperfine Nitrogen spectra for transitions $2p^2(^3P)\ 3s\ ^4P_J \rightarrow 2p^2(^3P)\ 3p\ ^4P_J^o$ and $^4D_J^o$. The proposed assignments for most of the weak lines observed by Cangiano et al. [4] and Jennerich et al. [1] are built on the hypothesis of crossovers signals appearing with intensities comparable to the expected (weak) real transitions, while the latter do not appear in the experimental spectra. This suggests strong perturbations in the recorded spectra, making the signals corresponding to weak transitions less intense than expected.

The possibility of an improper assignment of hyperfine components was ruled out by Jennerich et al. [1] by the fact that “the fits shown in Figure 2 are so good², and the resulting transition strength ratios are very close to the theoretical values”. On the other hand, for the transitions $^4P_{1/2} \rightarrow ^4P_{3/2}^o$ and $^4P_{3/2} \rightarrow ^4P_{5/2}^o$, the original analysis [1] called for strong line shape perturbations for explaining the non-observation of the expected resolved hyperfine structures for some transitions (one or two of the hyperfine components of a given transition becoming dominant, and the others becoming negligible in strength). The robustness of the present interpretation of the hyperfine spectra lies in the very good agreement of the present

model with the observed non-resolved spectra for the latter transitions. Moreover, while systematic large theory-observation discrepancies appeared for the relevant hyperfine parameters [2], the present analysis provides an experimental estimation (from the same spectra) of the hyperfine parameters in very good agreement with the *ab initio* results.

Non-linearities in the line intensities ratios are to be expected in saturated absorption spectroscopy. Even if the experimental setup can often be adapted to permit an unambiguous assignment of the spectra, we showed that this ambiguity can persist or, worse, that the spectra can be misleading, even, and maybe more, in very simple spectra. In those situations, theoretical calculations are helpful in discriminating two probable scenarios.

The recorded spectra of Jennerich et al. [1] should be reinvestigated according to the present analysis to refine the new set of hyperfine constants set and associated uncertainties. A definitive confirmation of one set or another would be the observation of a signal that is predicted in one model, but not in the other. An alternative would be to show a crossover-like dependence of the weak lines intensities with the experimental setup.

Isotope shift values were extracted from Jennerich et al.’s spectra [1]. Significant variations of the IS within each multiplet were reported. The present analysis built on a substantial revision of the hyperfine line assignments washes out the J -dependency of SMS found for $3p\ ^4P^o$ and $3p\ ^4D^o$ multiplets. On the contrary, a somewhat large SMS J -dependency is deduced for the even parity $3s\ ^4P$ multiplet. This effect is enhanced by the strong non-relativistic mixing with $1s^2\ 2s\ 2p^4\ ^4P$, which depends strongly of the total atomic electronic momentum J once relativistic corrections are added.

² see Figures 1(d), 2(d), 3(b,e), 4(b,e) in the present paper

Table 1. Comparison between the original experimental [1] and the *ab initio* [2] hyperfine constants with the new experimental values determined from the present analysis. All values are in MHz.

State	¹⁵ N			¹⁴ N					
	exp. [1] <i>A</i>	theory [2] <i>A</i>	exp. (this work) <i>A</i>	exp. [1] <i>A</i>	<i>B</i>	theory [2] <i>A</i>	<i>B</i>	exp. (this work) <i>A</i>	<i>B</i>
⁴ P _{1/2}	$\begin{cases} +103.4(14) \\ -153.1(23)^a \end{cases}$	-140.56	-153.1(23)	$\begin{cases} -69.76(90) \\ +112.3(13)^a \end{cases}$	0.0	100.21	0.0	+112.3(13)	0.0
⁴ P _{3/2}	-47.93(48)	-87.62	-95.86(96)	35.52(44)	-0.98(48)	62.46	4.10	68.33(69) ^b	3.5(91)
⁴ P _{5/2}	-90.71(71)	-175.12	-181.4(15)	64.76(42)	-3.9(10)	124.84	-5.12	129.52(84)	-7.8(20)
⁴ P _{1/2} ^o	167.1(13)	73.29	71.2(23)	-133.2(22)	0.0	-52.25	0.0	-50.78(17) ^b	0.0
⁴ P _{3/2} ^o	70.0(12)	-71.60	-66.1(23)	-48.56(74)	8.69(87)	51.04	-2.95	46.2(15)	-2.7(17)
⁴ P _{5/2} ^o	46.20(74)	-46.52	-44.5(15)	-32.83(44)	5.0(11)	33.16	2.57	31.93(86)	1.1(21)
⁴ D _{1/2} ^o	$\begin{cases} +153.1(23) \\ -103.4(14)^a \end{cases}$	-104.02	-103.4(14)	$\begin{cases} -112.3(13) \\ +69.76(90)^a \end{cases}$	0.0	74.15	0.0	+69.76(90)	0.0
⁴ D _{3/2} ^o	92.4(17)	-44.49	-43.7(28)	-64.41(79)	10.46(88)	31.71	0.30	30.3(15)	-0.9(17)
⁴ D _{5/2} ^o	41.5(14)	-51.57	-49.2(22)	-28.19(62)	-0.2(15)	36.76	-1.69	36.6(11)	-4.1(25)
⁴ D _{7/2} ^o	-9.35(55)	-78.04	-77.4(11)	6.31(72)	-12.6(13)	55.63	-6.44	55.2(11)	-9.9(26)

^a Second proposition of Jennerich et al. [1] (see text).^b Values taken from the constraint $A(^{15}\text{N})/A(^{14}\text{N}) = -1.4028$.

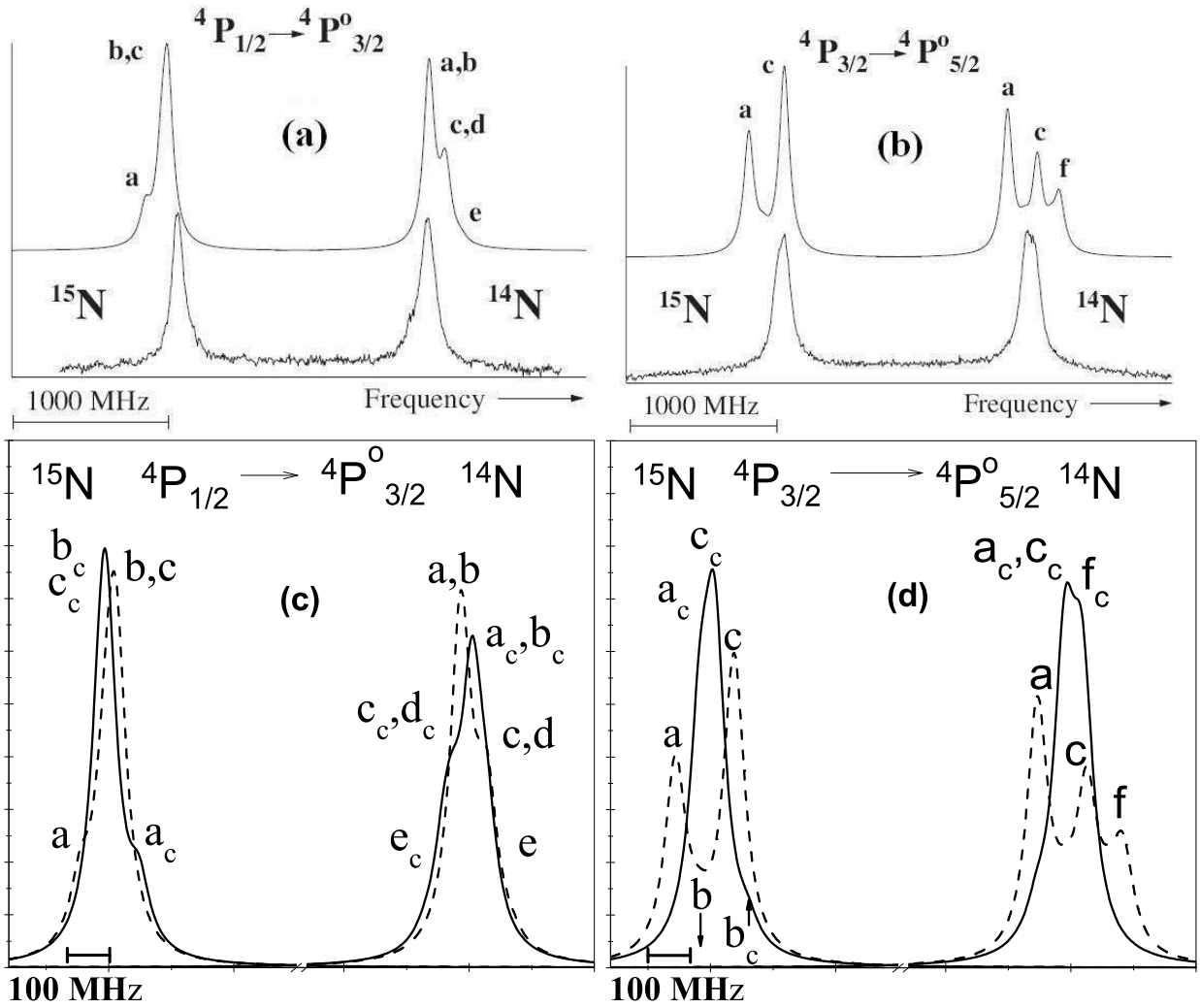


Fig. 7. Simulated and recorded spectra of the transitions $4P_{1/2} \rightarrow 4P_{3/2}^o$ and $4P_{3/2} \rightarrow 4P_{5/2}^o$ of ^{15}N and ^{14}N . Figures (a) and (c) are taken from Jennerich et al. [1], the lower spectra being the recorded ones. In Figures (c) and (d), the plain line corresponds to the \mathcal{S}_c simulations (transitions labels with indices c), without the crossover, and the dashed line corresponds to the \mathcal{S} spectra simulations using the experimental hyperfine constants. The latter differ from the simulations of Figures (a) and (c) by the used linewidth. The simulations are superposed on the same scale with the center of gravity of each spectra being at the origin (*i.e.* not including the $\delta\nu_0$ shift).

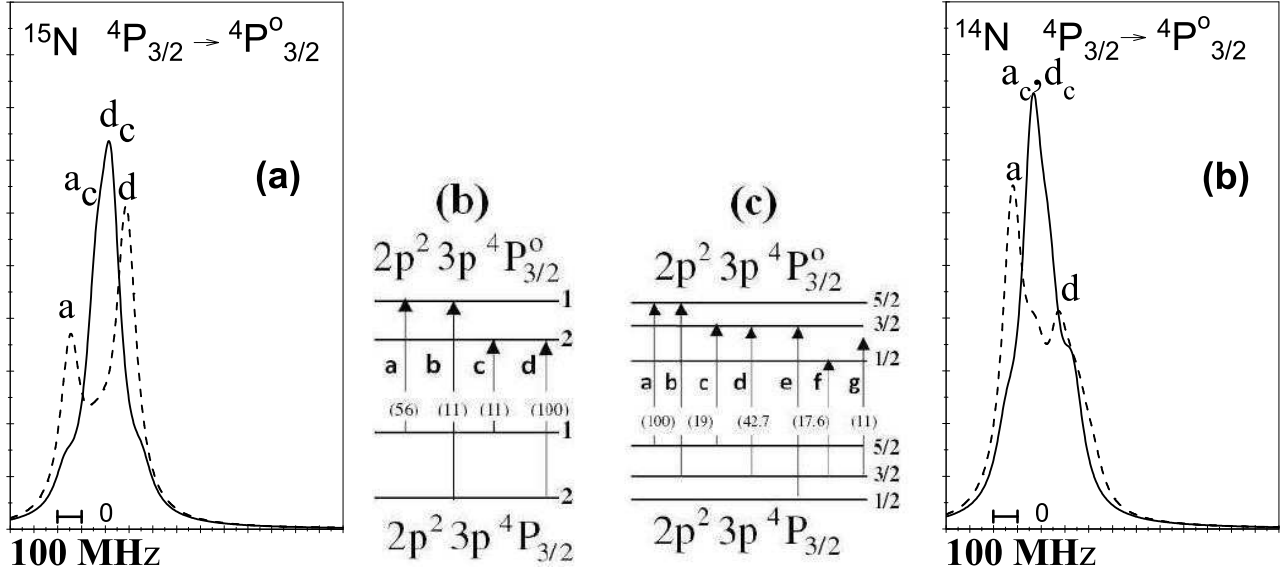


Fig. 8. Simulated and spectra of the transitions $4P_{3/2} \rightarrow 4P_{3/2}^o$ of ^{15}N and ^{14}N and corresponding level diagrams using Jennerich et al. assignment [1]. The plain line correspond to the S_c simulation (transitions labels with indices c), without the crossover, and the dashed line correspond to the S spectrum simulation using the experimental hyperfine constants. The simulations are superposed on the same scale with the center of gravity of each spectra being at the origin (*i.e.* not including the $\delta\nu_0$ shift).

Acknowledgements

TC is grateful to the “Fonds pour la formation la Recherche dans l’Industrie et dans l’Agriculture” of Belgium for a PhD grant (Boursier F.R.S.-FNRS). MG thanks the Communauté française of Belgium (Action de Recherche Concertée) and the Belgian National Fund for Scientific Research (FRFC/IISN Convention) for financial support. PJ acknowledges financial support from the Swedish Research Council.

References

1. R. Jennerich, A. Keiser, D. Tate, Eur. Phys. J. D **40**, 81 (2006)
2. P. Jönsson, T. Carette, M. Nemouchi, M. Godefroid, J. Phys. B: At. Mol. Opt. Phys. (2010), in press; arXiv:1002.4973v2 [physics.atom-ph]
3. J. Holmes, Phys. Rev. **43**, 41 (1943)
4. P. Cangiano, M. de Angelis, L. Gianfrani, G. Pesce, A. Sasso, Phys. Rev. A **50**, 1082 (1994)
5. W. Demtröder, *Laser Spectroscopy* (Springer, 2008)
6. T.W. Hänsch, I.S. Shahin, A.L. Schawlow, Phys. Rev. Lett. **27**, 707 (1971)
7. C. Anderson, J. Lawler, T. Holley, A. Filippelin, Phys. Rev. A **17**, 2099 (1978)
8. S. Krins, S. Oppel, N. Huet, J. von Zanthier, T. Bastin, Phys. Rev. A **80**, 062508 (2009)
9. R.S. Gurjar, K.K. Sharma, Phys. Rev. A **59**, 512 (1999)
10. L. Sangkyung, L. Kanghee, A. Jaewook, Japanese Journal of Applied Physics **48**, 032301 (2009)
11. K.B. Im, H.Y. Jung, C.H. Oh, S.H. Song, P.S. Kim, Phys. Rev. A **63**, 034501 (2001)
12. P. Pappas, M. Burns, D. Hinshelwood, M. Feld, Phys. Rev. A **21**, 1955 (1980)
13. H. Rinneberg, T. Huhle, E. Matthias, A. Timmermann, Z. Phys.A–Atoms and Nuclei **295**, 17 (1980)
14. R. Grimm, J. Mlynek, Appl. Phys. B **49**, 179 (1989)
15. O. Schmidt, K.M. Knaak, R. Wynands, R. Meschede, Appl. Phys. B **59**, 167 (1994)
16. A. Sargsyan, D. Sarkisyan, A. Papoyan, Y. Pashayan-Leroy, P. Moroshkin, A. Weis, A. Khanbekyan, E. Mariotti, L. Moi, Laser Physics **18**, 749 (2008)
17. A. Banerjee, V. Natarajan, Opt. Lett. **28**, 1912 (2003)
18. R.D. Cowan, *The Theory of Atomic Structure and Spectra*, Los Alamos Series in Basic and Applied Sciences (University of California Press, 1981)
19. N. Stone, At. Data Nucl. Data Tables **90**, 75 (2005)
20. A. Hibbert, Rep. Prog. Phys. **38**, 1217 (1975)
21. D. Tate, J. Walton, Phys. Rev. A **59**, 1170 (1999)
22. R. Jennerich, D. Tate, Phys. Rev. A **62**, 042506 (2000)
23. A. Hibbert, E. Biémont, M. Godefroid, N. Vaeck, J. Phys. B : At. Mol. Phys. **24**, 3943 (1991)